

Role of carboxylate ion and metal oxidation state on the morphology and magnetic properties of nanostructured metal carboxylates and their decomposition products[†]

APARNA GANGULY^b, RITUPARNA KUNDU^a, KANDALAM V RAMANUJACHARY^c, SAMUEL E LOFLAND^d, DIPANKAR DAS^c, N Y VASANTHACHARYA^f, TOKEER AHMAD^b and ASHOK K GANGULI^{a*}

^aDepartment of Chemistry, Indian Institute of Technology, Hauz Khas, New Delhi 110 016

^bDepartment of Chemistry, Faculty of Natural Sciences, Jamia Millia Islamia, New Delhi 110 025

^cDepartment of Chemistry and Biochemistry, Center for Materials Research and Education, Rowan University, 201 Mullica Hill Road, Glassboro, NJ 08028, USA

^dDepartment of Physics, Center for Materials Research and Education, Rowan University, 201 Mullica Hill Road, Glassboro, NJ 08028, USA

^eUGC-DAE, Consortium for Scientific Research, LB-8, Sector-III, Bidhannagar, Kolkata 700 098

^fSolid State and Structural Chemistry Unit, Indian Institute of Sciences, Bangalore 560 012
e-mail: ashok@chemistry.iitd.ernet.in

Abstract. Sub-micron rods and spheres of cobalt succinate sesquihydrate and iron succinate trihydrate/pentahydrate respectively have been synthesized by the reverse micellar route. These precursors are an excellent source for the synthesis of metal and metal oxide nanoparticles. Cubes of (edge length ~ 150 nm) Fe₃O₄ and elongated particles of Fe₂O₃ (~ diameter of 200 nm) were obtained. The role of oxidation state of the metal ion in controlling the morphology of the nanostructured dicarboxylates has been investigated. Rods with shorter length were obtained when longer chain dicarboxylate was used as ligand. Heating in nitrogen atmosphere also provided pure Co and α -Fe nanoparticles. The Fe nanoparticles show nearly 100% superparamagnetism. Temperature-dependent magnetic studies show a Morin-like transition for Fe₂O₃ nanoparticles at 223 K and the Verwey transition at 115 K for Fe₃O₄ nanoparticles. Co₃O₄ nanoparticles showed antiferromagnetic ordering at 20 K.

Keywords. Reverse micelles; Morin transition; metal carboxylates; Verwey transition.

1. Introduction

Hybrid inorganic–organic compounds are attracting interest as a class of materials that are well-suited for the incorporation of transition metal ions, especially in inorganic solids having porous networks. The use of organic moieties to build extended metal–organic nanostructures is currently being investigated on a large scale. These are found to be promising materials for applications in catalysis, separation, gas storage and molecular recognition. Several studies on single crystals of three-dimensional open framework structures complexed with metal ions obtained by hydrothermal method have been reported.^{1,2} Kinetic analysis on the thermal decompo-

sition of transition metal succinates obtained by coprecipitation method has also been reported,³ which led to either single crystalline (0.01 mm) or micron-sized polycrystalline materials. We have been interested in the nanostructures of metal–organic-based systems. Earlier we have obtained nanorods of metal oxalates of several metals using the reverse micellar route.^{4–6} Reverse micelles have been widely used for the preparation of a variety of nanoparticles due to their ability to mix the reactants efficiently and to control the size of the nanoparticles. Here we use the succinate moiety to generate metal succinate nanostructures using the reverse micellar method.

These succinate metal–organic precursors were decomposed under different atmospheres to obtain pure metal and metal–oxide nanoparticles. We could obtain fine nanoparticles of maghemite, α -Fe₂O₃, and magnetite, Fe₃O₄, by varying the conditions of

[†]Dedicated to Prof. C N R Rao on his 75th birthday

*For correspondence

decomposition of the succinate. We have also obtained nanoparticles of Co_3O_4 which is an important oxide used for electrochemical, magnetic and catalytic applications. We compared the magnetic properties of the metal succinate precursors and the oxide nanoparticles with those obtained by using metal oxalates as precursors.⁴

2. Experimental

Water soluble $\text{Co}(\text{NO}_3)_2 \cdot 6\text{H}_2\text{O}$, $\text{Fe}(\text{NO}_3)_3 \cdot 9\text{H}_2\text{O}$ and $\text{FeCl}_2 \cdot 4\text{H}_2\text{O}$ were used as the metal ion sources. Microemulsion systems were prepared with CTAB as the surfactant, 1-butanol as the co-surfactant and isooctane as the hydrocarbon phase. Two microemulsions, one containing the metal ion and the other containing the succinate ion were mixed slowly. The product was collected by centrifugation and washed with a mixture of organic solvents to remove the surfactant and was allowed to dry at room temperature. Apart from the above synthesis using $\text{Fe}(\text{NO}_3)_3 \cdot 9\text{H}_2\text{O}$ and $\text{Co}(\text{NO}_3)_2 \cdot 6\text{H}_2\text{O}$, we also carried out a similar reaction using iron (II) chloride tetrahydrate as the starting reagent.

Powder X-ray diffraction (PXRD) studies were carried out on a Bruker D-8 Advance X-ray diffractometer using Ni filtered $\text{CuK}\alpha$ radiation. Normal scans were recorded with a step of 0.02° and a residence time of 1 s. Infrared (IR) spectra of the succinates and oxides were recorded in the transmission mode in the range of $200\text{--}4000\text{ cm}^{-1}$ on a Nicolet Protégé 460 Fourier-transform infrared (FTIR) spectrometer with KBr discs. Thermogravimetric analysis (TGA) and differential Thermal analysis (DTA) were carried out on a Perkin-Elmer TGA-DTA instrument. Well-ground and dry samples were loaded under flowing nitrogen with a heating rate of $5^\circ/\text{min}$. High resolution transmission electron microscopy (TEM) was recorded on a Technai G² 20 (FEI) electron microscope operated at 200 kV. TEM specimens were prepared by loading a drop of the ultrasonically dispersed sample in ethanol on a carbon-coated copper grid and dried in air. Magnetization studies of the metal succinates and the metal oxides were measured at temperatures ranging from 5 to 300 K, in applied fields of up to 10 kOe with a Quantum Design Physical Properties Measurement System. Magnetisation studies for Fe nanoparticles were carried out on a Lakeshore Model 7400 VSM. Mössbauer measurements were carried out at room temperature with a 512-channel Mössbauer spec-

trometer operating in constant acceleration mode. A 10 mCi ^{57}Co in Rh matrix was used as the radioactive source. The spectrometer was calibrated with a $12\ \mu\text{m}$ thick natural iron foil of high purity.

3. Results and discussion

PXRD patterns of the as-prepared metal succinates showed the amorphous nature of these compounds. The samples were heated up to 200°C in stages to improve the crystallinity, but no significant change was observed in the PXRD pattern. The complexation of the metal to the ligand was confirmed by the characteristic IR bands. Bands corresponding to $3700\text{--}2850\text{ cm}^{-1}$ (presence of O–H bond), 1599 cm^{-1} (C=O group), 670 cm^{-1} (Co–O) and 560 cm^{-1} (Fe–O) were observed.

TEM studies of cobalt succinate dihydrate showed rods of $\sim 500\text{ nm}$ length and 50 nm diameter (figure 1). In our earlier reports,^{4–6} we found that almost all metal oxalates, prepared by a similar reverse micellar route led to M (II) oxalates with rod-like structures except for cerium oxalate⁷ where we observed spherical particles.

TEM studies of iron (III) succinate synthesized from $\text{Fe}(\text{NO}_3)_3 \cdot 9\text{H}_2\text{O}$ showed spherical particles of size $\sim 150\text{--}200\text{ nm}$ (figure 2a). Mössbauer study was carried out to confirm the oxidation state (O.S.) of

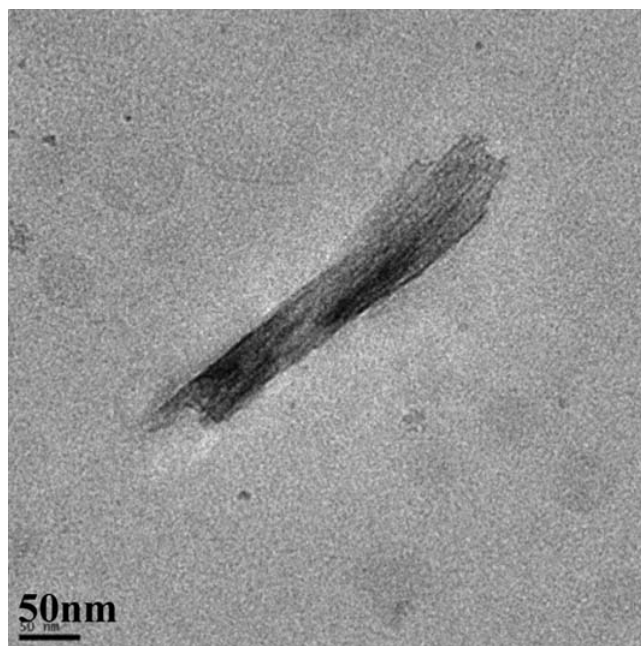


Figure 1. TEM micrograph of cobalt succinate dihydrate at room temperature.

Fe (figure 2b). The isomer shift values are consistent with trivalent iron in octahedral geometry. It is thus expected that due to the +III O.S. of the metal ion, the ratio of metal ion to ligand required for charge neutralization would be 2 : 3. This ratio of metal to ligand results in the formation of spherical particles instead of a rod-like structure, which would normally require a 1 : 1 ratio of metal ion : ligand as shown in earlier studies on metal oxalates^{4,8}.

In an attempt to further investigate the role of oxidation state of the metal ion, we used $\text{FeCl}_2 \cdot 4\text{H}_2\text{O}$ as the starting reagent instead of $\text{Fe}(\text{NO}_3)_3$. The PXRD pattern and IR spectrum of the metal succi-

nate were found to be similar to that obtained with $\text{Fe}(\text{NO}_3)_3$. The TEM studies show smaller spherical particles of size $\sim 20\text{--}30\text{ nm}$ (figure 3a). Mössbauer studies confirmed the presence of trivalent O.S. of Fe (figure 3b). The large quadrupole splitting (QS) values show significant distortion of the octahedra around Fe atom. From the above studies it appears that though the metal ion was initially in the +2 O.S. (FeCl_2), it gets oxidized during the preparation of the microemulsion or during the reaction when the two microemulsions were mixed.

The TGA/DTA studies for cobalt succinate in flowing nitrogen shows two sharp weight losses at 130°C and at 415°C . The first weight loss at 130°C

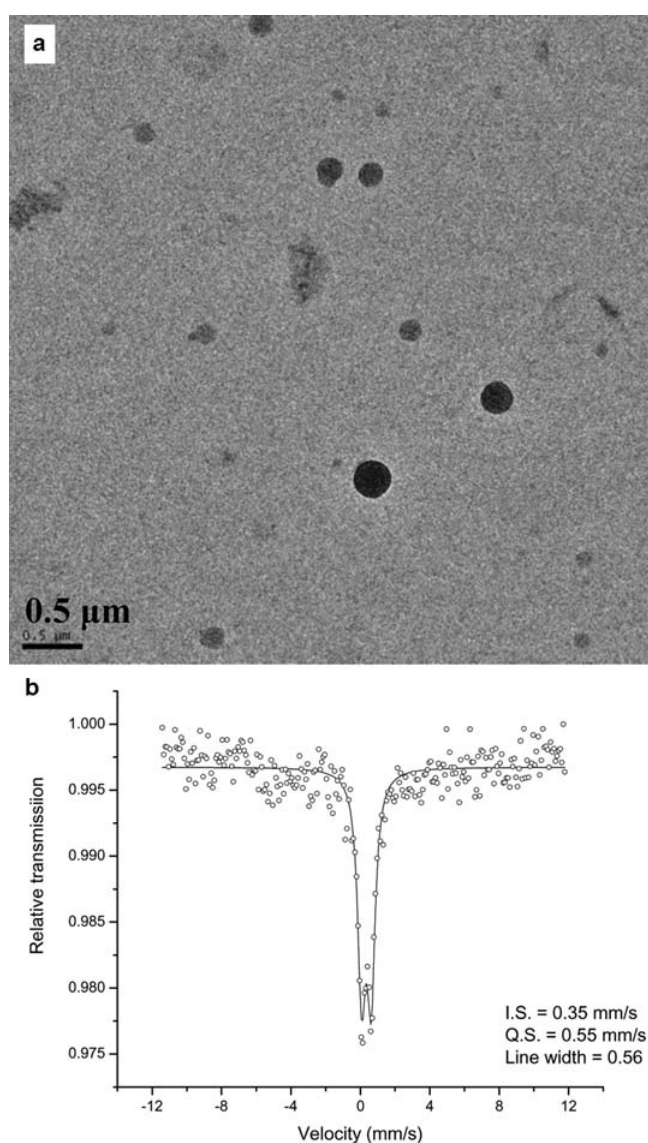


Figure 2. (a) TEM of iron succinate and (b) Mössbauer spectra of iron succinate synthesized using $\text{Fe}(\text{NO}_3)_3 \cdot 9\text{H}_2\text{O}$ at room temperature.

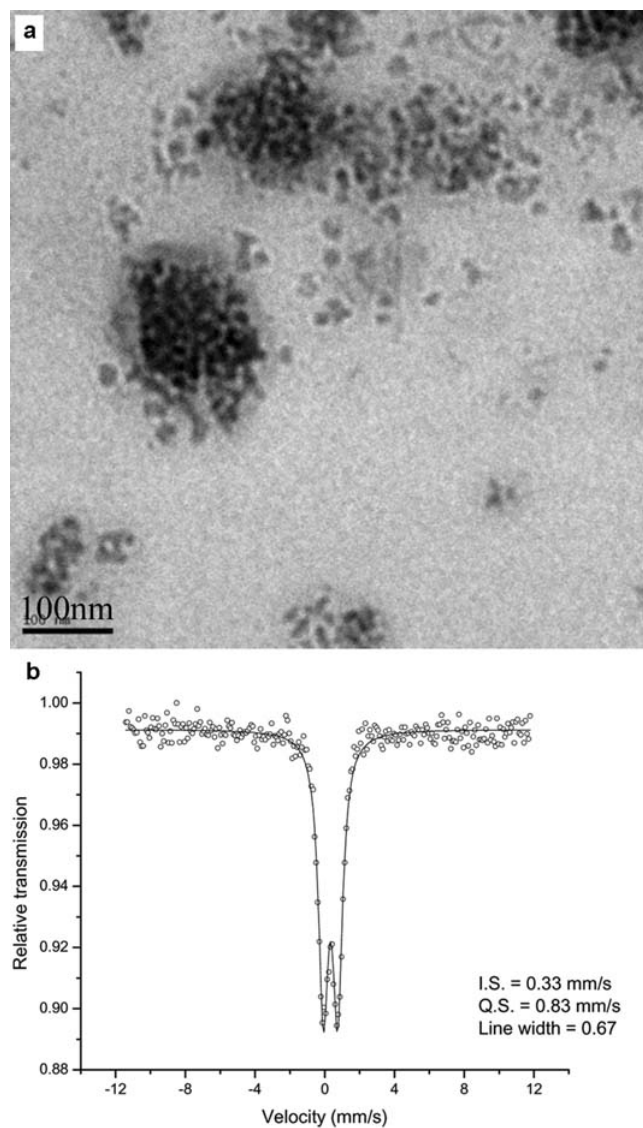


Figure 3. (a) TEM of iron succinate and (b) Mössbauer spectra of iron succinate synthesized using $\text{FeCl}_2 \cdot 4\text{H}_2\text{O}$.

corresponds to the loss of one-and-half water molecules. The final weight loss corresponds to the decomposition of cobalt succinate to cobalt nanoparticles. However, the final product was also found to contain some unburnt carbon residue. This is in accordance with the data as obtained by Muraishi *et al* in their detailed thermal analysis of metal succinates.⁹ Cobalt succinate dihydrate heated at 500°C for 6 h in air yielded pure Co_3O_4 (figure 4). All the reflections in the PXRD pattern could be indexed on the basis of a cubic cell for Co_3O_4 with refined lattice parameters of $a = 8.069(3)$ Å. The crystallite size of Co_3O_4 nanoparticles was found to be ~ 53 nm by Scherrer's formula while TEM of the same sample shows particles of ~ 50 – 60 nm (figure 5a) and the lattice fringes could be indexed as (222) planes (figure 5b). In the presence of nitrogen at 650°C, cobalt succinate dihydrate decomposed to yield pure Co nanoparticles (figure 6) with size ranging between 10 and 40 nm (figure 7).

For iron (III) succinate synthesized from $\text{Fe}(\text{NO}_3)_3 \cdot 9\text{H}_2\text{O}$, two weight losses were observed in TGA (under nitrogen) at 100°C and at 350°C. The weight loss at 100°C corresponds to the loss of 3 moles of water suggesting that a trihydrate complex had formed. From the TGA plot, formation of metal oxides was found to be around 415°C. Hence, the sample was subjected to heat treatment in the range of 375 to 500°C under different atmospheric conditions (air and nitrogen). It was found that when heated in the presence of air at 375°C, iron succinate gives $\alpha\text{-Fe}_2\text{O}_3$ (figure 8a), yielding cubes of edge length ~ 180 nm and some elongated particles of size ~ 150 nm (figure 8b). In the presence of nitrogen at

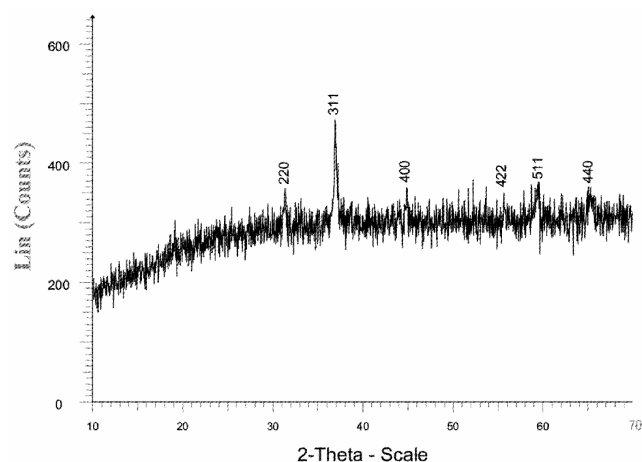


Figure 4. PXRD of Co_3O_4 obtained by heating cobalt succinate at 500°C in air.

500°C it produces a mixture of Fe_3O_4 and Fe (figure 9a) with Fe_3O_4 nanoparticles with edge length ~ 50 nm (figure 9b). Earlier thermal studies on iron (II) oxalate dihydrate showed sharp transitions at 160 and 410°C which led to Fe_2O_3 nanoparticles of size ~ 50 nm joined together to form Y-junctions in air and faceted grains of Fe_3O_4 of size ~ 60 – 70 nm when heated in vacuum.

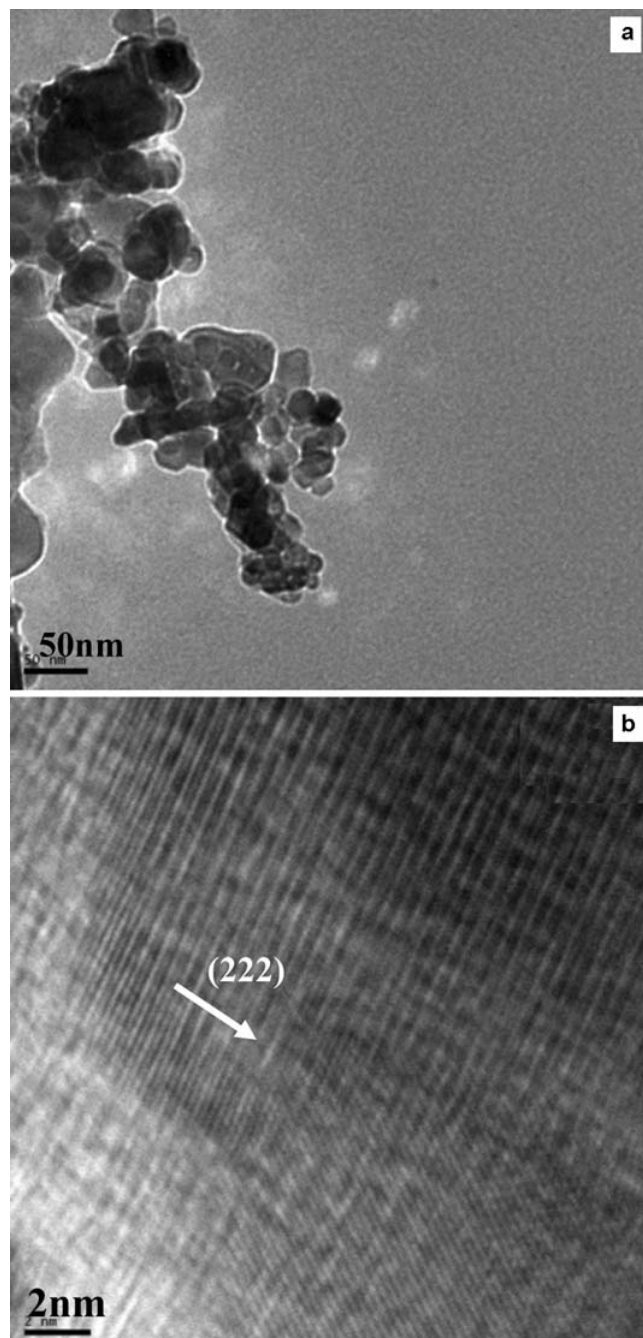


Figure 5. (a) TEM micrograph of Co_3O_4 nanoparticles at 500°C and (b) HRTEM of Co_3O_4 .

Iron succinate synthesized from $\text{FeCl}_2 \cdot 4\text{H}_2\text{O}$ shows a gradual decomposition up to 1000°C in nitrogen with broad transitions at 200 , 450 and 970°C suggesting a loss of 5 moles of water, and the final product corresponds to formation of elemental iron along with some carbon residue. In the presence of nitrogen, the succinate precursor was found to decompose at 800°C to pure $\alpha\text{-Fe}$ (bcc) nanoparticles (figure 10).

We have studied the magnetic properties of the metal succinate and their oxides. Antiferromagnetic-type behaviour is observed from the susceptibility

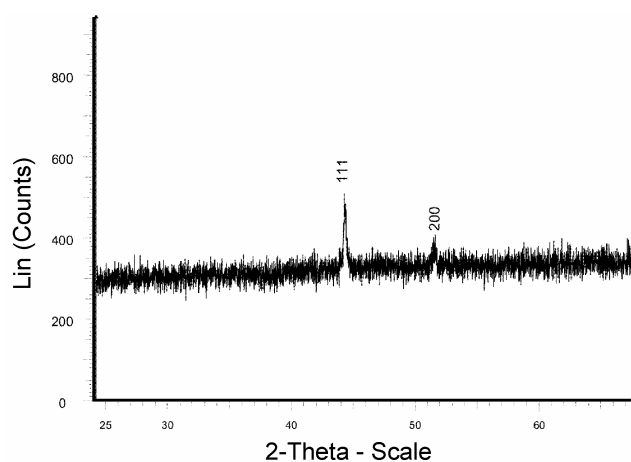


Figure 6. PXRD pattern of Co nanoparticles obtained by heating cobalt succinate at 650°C under nitrogen.

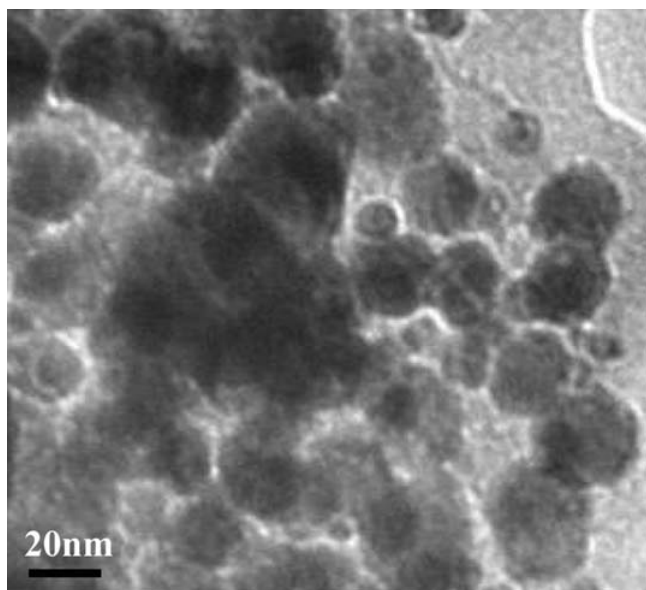


Figure 7. TEM micrograph of Co nanoparticles obtained by heating the cobalt succinate at 650°C under nitrogen.

plots of cobalt succinate dihydrate (figure 11). The effective magnetic moment μ_{eff} calculated from the Curie plot in the range of $100\text{--}300\text{ K}$ is found to be 5.9 Bohr magnetons (B.M.), which is higher than the theoretical value of 3.87 B.M for Co^{2+} . Presumably, the rise at low temperature is due to Curie impurities.

Co_3O_4 has a normal spinel structure with Co^{2+} occupying the tetrahedral position and the Co^{3+} ion occupying the octahedral position. Since in its low spin configuration, Co^{3+} ($t_{2g}^6 e_g^0$) does not contribute to the magnetic moment, the measured susceptibility arises due to the divalent ion with a d^7 configuration ($t_{2g}^5 e_g^2$). The observed high value of μ_{eff} (8.34 B.M.)

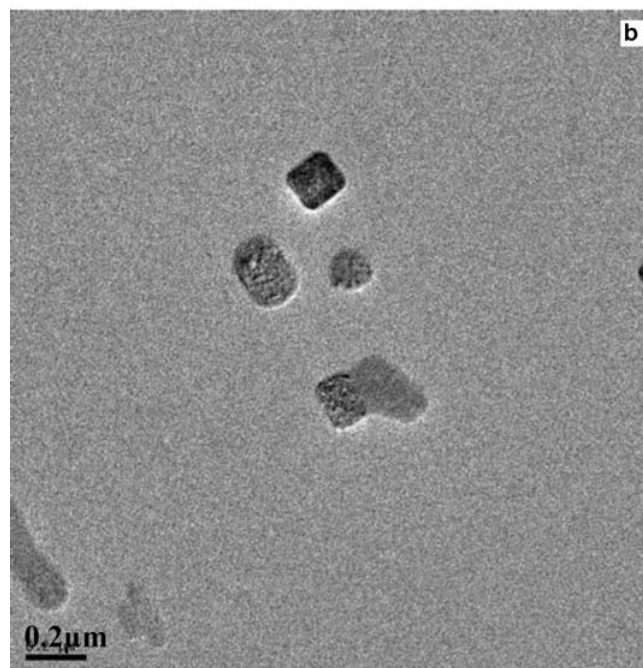
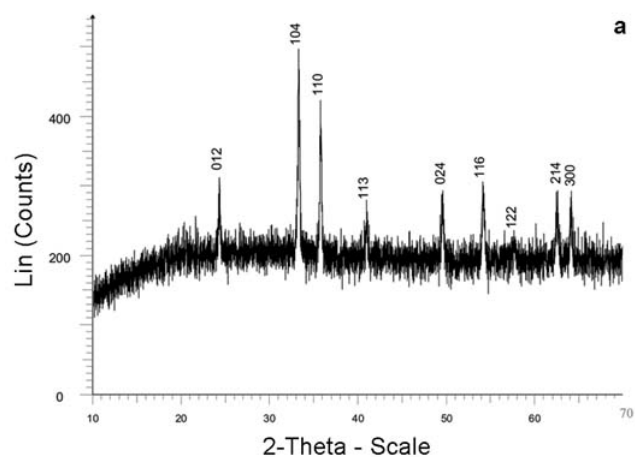


Figure 8. (a) PXRD pattern and (b) TEM micrograph of $\alpha\text{-Fe}_2\text{O}_3$ nanoparticles obtained by decomposing Fe(III) succinate at 375°C in air.

has been observed in Co_3O_4 nanoparticles by Yamada *et al.*,¹¹ who attributed it to uncompensated superparamagnetic surface spins and the presence of oxygen defects. Antiferromagnetic ordering occurs at ~ 20 K (figure 12). Note that such a transition is reported at ~ 33 K for the bulk compound.

Fe(III) succinate synthesized from $\text{FeCl}_2 \cdot 4\text{H}_2\text{O}$ shows antiferromagnetic behaviour. The magnetic moment calculated (5.9 B.M.) matches well with the theoretical value (5.9 B.M.) which also corroborates with the Mössbauer studies (figure 13). It is to be noted that electron spin resonance spectra (not shown) display two lines, suggesting more than one Fe site or valence. More detailed structural studies are re-

quired to understand the arrangement of the Fe^{3+} in the lattice. The susceptibility of Fe(III) succinate

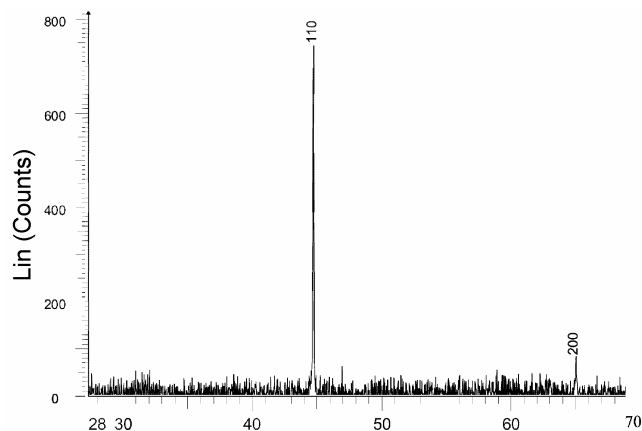


Figure 10. PXRD pattern of Fe obtained by decomposing iron succinate at 800°C in nitrogen.

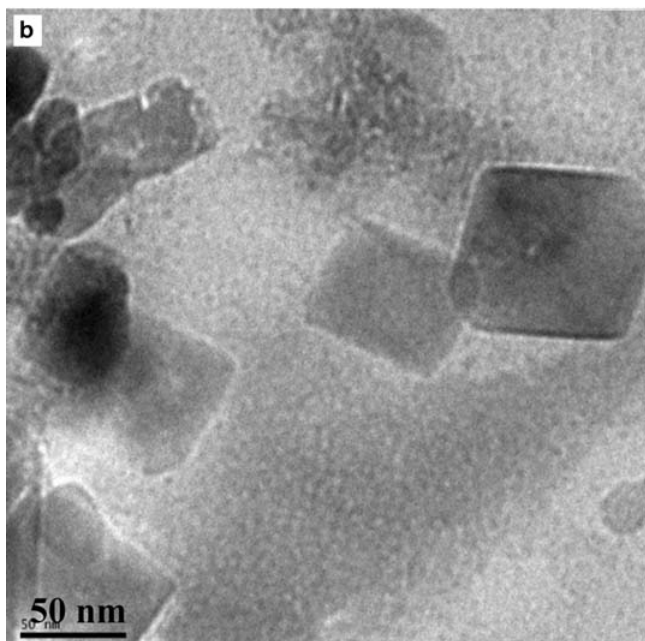
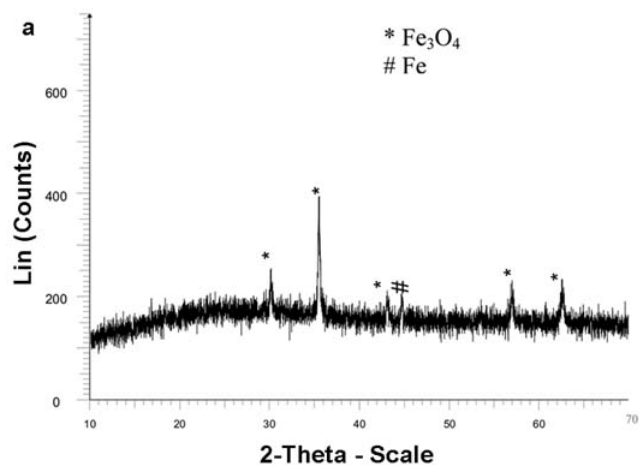


Figure 9. (a) PXRD pattern and (b) TEM micrograph of Fe_3O_4 obtained by decomposing Fe(III) succinate at 500°C in nitrogen.

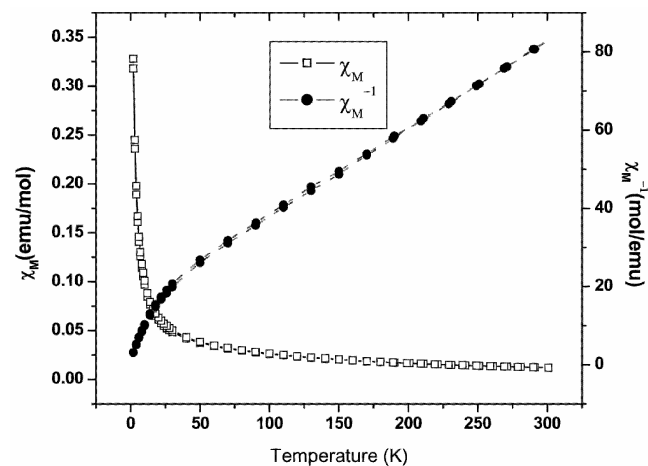


Figure 11. Temperature variation studies of magnetic susceptibility and inverse magnetic susceptibility of cobalt succinate dihydrate.

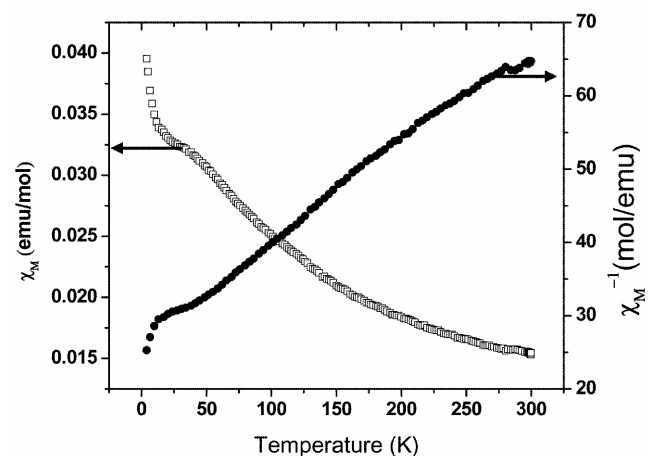


Figure 12. Temperature variation studies of magnetic susceptibility and inverse magnetic susceptibility of Co_3O_4 at 0.1 T.

synthesized from $\text{Fe}(\text{NO}_3)_3$ also showed antiferromagnetic behaviour (figure 14) although there is an anomalous increase below 50 K. The magnetic moment as calculated from the Curie plot (4.41 B.M.) is lower than that of the calculated theoretical value (5.9 B.M.), assuming Fe^{3+} .

The nano-cubes of $\alpha\text{-Fe}_2\text{O}_3$, with edge length of ~ 150 nm, show a weak antiferromagnetic ordering (figure 15) at around 223 K which is reminiscent of the Morin transition. $\alpha\text{-Fe}_2\text{O}_3$ single crystals have been reported to show the Morin transition (T_m) from a weakly ferromagnetic solid to a weakly antiferromagnetic solid below 263 K.¹² The T_m shifts to lower temperatures with decrease in particle size which may be due to lattice defects and strains in the small-sized particles. Similar type of transition was

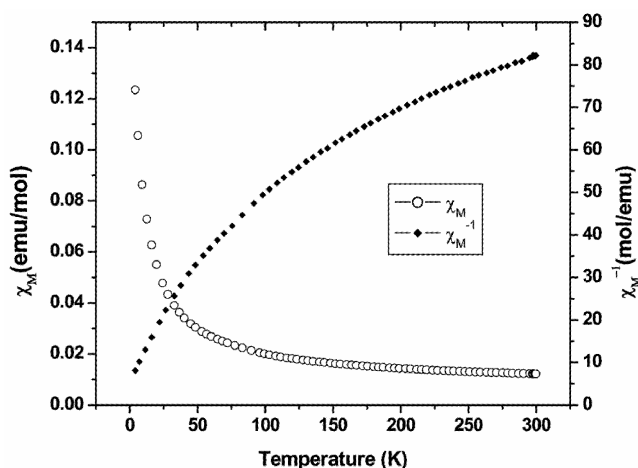


Figure 13. Temperature variation studies of magnetic susceptibility and inverse magnetic susceptibility of iron succinate synthesized using $\text{FeCl}_2 \cdot 4\text{H}_2\text{O}$.

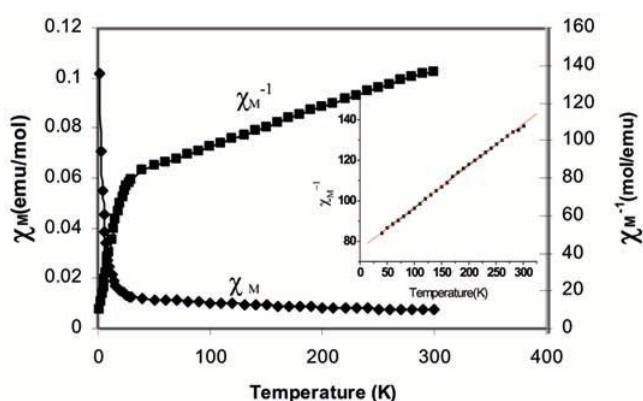


Figure 14. Temperature variation studies of magnetic susceptibility iron succinate trihydrate synthesized using $\text{Fe}(\text{NO}_3)_3 \cdot 9\text{H}_2\text{O}$. Inset shows the inverse plot of susceptibility vs temperature.

observed at 225 K for the Fe_2O_3 nanoparticles obtained from iron oxalate.⁴

Fe_3O_4 nanoparticles showed a magnetic transition at ~ 115 K (figure 15b). This Verwey transition occurs in bulk Fe_3O_4 at 120 K.¹³ The transition was observed in the case of Fe_3O_4 nanoparticles obtained from iron oxalate at 122 K.⁴

The magnetization studies of the Fe nanoparticles show a magnetization of more than 45 emu/g at room temperature, negligible hysteresis and a lack of saturation, which suggest nearly superparamagnetic behaviour (figure 16).

In comparison to our earlier reports^{4,8} on the synthesis and characterization of metal oxalates, we could observe a distinct change in morphology of the product from nanorods to nanoparticles as we changed the carboxylate anion from oxalate to succinate. Nanorods of iron oxalate dihydrate with an aspect ratio of ~ 7 were obtained from oxalates⁴ while only spherical nanoparticles of iron succinate could be synthesized. From the Mössbauer studies, it was confirmed that iron in both the succinate complexes was in trivalent state and hence the formation of nanorods is not favourable.⁸ However, for both the oxalate and succinate precursors of cobalt, nanorods were observed. With the oxalate ligand, mi-

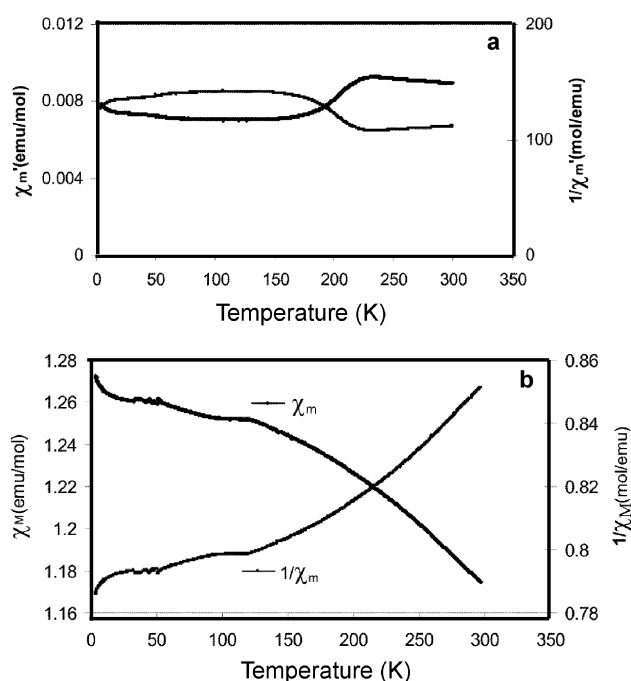


Figure 15. Temperature variation studies of magnetic susceptibility and inverse magnetic susceptibility (a) $\alpha\text{-Fe}_2\text{O}_3$ and (b) Fe_3O_4 .

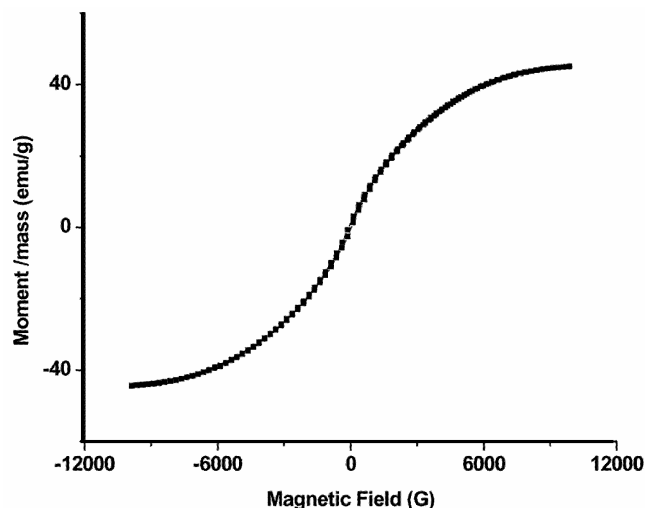


Figure 16. Hysteresis loop for nanoparticles of Fe at 300 K.

ron-sized rods were formed¹⁴ while with the succinate anion, shorter rods of few hundred nanometers and 50 nm diameter were found. Note that in case of bulk cobalt succinate, a dimeric structure is known where the carboxylate group is bonded to two different cobalt atoms to give a tetrahedral environment.³ This structural necessity probably leads to shorter rods. Thus it seems that the bidentate succinate ion also favours the formation of rods like the oxalate ion only if the metal ion is in +2 oxidation state as evidenced from the formation of cobalt succinate nanorods.

4. Conclusions

Polycrystalline metal–organic hybrid nanostructures were made by the reverse micellar route. Controlled thermal treatment of the succinate precursors under different atmospheric conditions yielded metal and metal-oxide nanoparticles. We find a significant change in particle size for the spherical nanoparticles of iron succinate as we change the reactant metal ion from $\text{Fe}(\text{NO}_3)_3 \cdot 9\text{H}_2\text{O}$ (150–200 nm) to $\text{FeCl}_2 \cdot 4\text{H}_2\text{O}$ (20–30 nm). A change in the morphology of metal carboxylates was also observed when succinate was used instead of oxalate. Spherical nanoparticles were formed for iron succinate opposed to the nanorods we got for iron oxalate.⁴ Cobalt oxide (Co_3O_4) nanoparticles of size ~ 60 nm was

obtained from the succinate precursor which shows weak antiferromagnetic ordering at 20 K. Nanoparticles of $\alpha\text{-Fe}_2\text{O}_3$ obtained from iron succinate shows weak antiferromagnetic ordering (Morin transition) at 223 K which is much lower than that found in bulk Fe_2O_3 . Nanoparticles of Fe_3O_4 have faceted cuboidal shape with a weak Verwey-like transition at 115 K. In addition, a very simple route to obtain nearly 100% superparamagnetic $\alpha\text{-Fe}$ nanoparticles was developed from a succinate precursor.

Acknowledgements

AKG and TA thank the Department of Science and Technology (DST) and Council of Scientific and Industrial Research (CSIR), Government of India for financial support. AG thanks University Grants Commission (UGC) for a fellowship. Thanks to Ms B Bhushan for the analysis of Mössbauer data. SEL acknowledges support from National Foundation of Science (NSF) MRSEC DMR 0520471. KVR appreciates the support of DST, Government of India for the award of a CP-STIO fellowship.

References

1. Livage C, Egger C and Ferey G 1999 *Chem. Mater.* **11** 1546
2. Vaidhyanathan R, Natarajan S and Rao C N R 2002 *Inorg. Chem.* **41** 5226
3. Abd El-Salaam K M, Halawani K H and Fakiha S A 1992 *Thermochimica Acta* **204** 311
4. Ganguli A K and Ahmad T 2007 *J. Nanosci. Nanotech.* **7** 2029
5. Ahmad T, Ramanujachary K V, Lofland S E and Ganguli A K 2004 *J. Mater. Chem.* **14** 3406
6. Ahmad T, Vaidya S, Sarkar N, Ghosh S and Ganguli A K 2006 *Nanotechnology* **17** 1236
7. Vaidya S, Ahmad T, Agarwal S and Ganguli A K 2007 *J. Am. Ceram. Soc.* **90** 863
8. Ahmad T, Chopra R, Ramanujachary K V, Lofland S E and Ganguli A K 2005 *J. Nanosci. Nanotech.* **5** 1840
9. Yokobayashi H, Nagase K and Muraishi K 1975 *Bull. Chem. Soc. Jap.* **48** 2789
10. Roth W I 1964 *J. Phys. Chem. Solids* **25** 1
11. Ichiyangi Y and Yamada S 2005 *Polyhedron* **24** 2813
12. Morin F J 1950 *Phys. Rev.* **819**
13. Verwey E J W 1939 *Nature* **44** 327
14. Ahmed J, Ahmad T, Ramanujachary K V, Lofland S E and Ganguli A K 2008 *J. Colloid Interface. Sci.* **321** 434